HHS Public Access

Author manuscript

Mol Cancer Ther. Author manuscript; available in PMC 2018 July 01.

Published in final edited form as:

Mol Cancer Ther. 2017 July ; 16(7): 1257–1268. doi:10.1158/1535-7163.MCT-17-0115.

Co-targeting mTORC and EGFR signaling as a therapeutic strategy in HNSCC

Adam D. Swick[1], **Prashanth J. Prabakaran**[1], **Margot C. Miller**[1], **Amal M. Javaid**[1], **Michael M. Fisher**[1], **Emmanuel Sampene**[2], **Irene M. Ong**[2,4], **Rong Hu**[3], **Mari Iida**[1], **Kwangok P. Nickel**[1], **Justine Y. Bruce**[4,5], **Deric L Wheeler**[1,4], and **Randall J. Kimple**[1,4]

[1]Department of Human Oncology, University of Wisconsin School of Medicine, Madison, WI 53705, USA

[2]Department of Biostatistics and Medical Informatics, University of Wisconsin School of Medicine, Madison, WI 53705, USA

[3]Department of Pathology, University of Wisconsin School of Medicine, Madison, WI 53705, USA

[4]University of Wisconsin Carbone Cancer Center, University of Wisconsin School of Medicine, Madison, WI 53705, USA

[5]Department of Medicine, University of Wisconsin School of Medicine, Madison, WI 53705, USA

Abstract

Head and neck squamous cell carcinomas (HNSCCs) are frequently altered along the PI3K/AKT/mTORC signaling axis. Despite excellent preclinical data, the use of compounds targeting this pathway as monotherapy has been underwhelming in initial clinical trials and identification of predictive biomarkers remains challenging. To investigate mTORC specific inhibition we tested catalytic mTORC (AZD8055) and PI3K/mTORC (NVP-BEZ-235) inhibitors +/− cetuximab in a panel of HNSCC cell lines and patient derived xenografts (PDX). Cell lines were assayed for response to all agents and siRNA knockdown of targets by multiple approaches. All cell lines showed similar response to both drug and siRNA inhibition of both PI3K and mTORC pathways, with anti-EGFR combination producing modest additive effect. Five PDX models that presented PIK3CA mutation or intrinsic cetuximab resistance were treated with a combination of cetuximab and AZD8055. In vivo single agent mTORC inhibition inhibited growth of a PIK3CA mutant cancer, but had little effect on any $PIK3CA^{WT}$ or a second PIK3CA mutant model. In all models the combination therapy showed greater growth delay than monotherapy. The uniform ability of PI3K and mTORC inhibition to suppress the growth of HNSCC cells highlights the pathway's role in driving proliferation. While single agent therapy was largely ineffective in vivo, improved response of combination treatment in an array of PDXs suggests the potential for adding a catalytic mTORC inhibitor to cetuximab therapy. Overall, these results add to a growing body of evidence suggesting approaches that attempt to match biomarkers to the optimal therapy in HNSCC remains complex and challenging.

Corresponding author: Randall J. Kimple, MD PhD; Department of Human Oncology; University of Wisconsin Comprehensive Cancer Center; 3107 WIMR, 1111 Highland Avenue, Madison, WI 53792; Phone: (608) 265-9156; rkimple@humonc.wisc.edu; Twitter: @KimpleRandall.

Conflicts of interest: None

Keywords

Head and neck cancer; mTORC inhibition; EGFR therapy; patient derived xenograft

Introduction

Head and neck squamous cell carcinoma (HNSCC) remains a common and deadly disease with almost 60,000 new diagnoses and 13,000 deaths annually in the United States(1). While declining tobacco use in the US has reduced disease incidence, this has been partially offset by increases in human papillomavirus (HPV) driven cancers(2–5), resulting in the need for improved treatment of HNSCC for the foreseeable future. The high frequency of EGFR overexpression in HNSCC led to the use of the EGFR-targeting monoclonal antibody cetuximab for the treatment of this disease(6,7). While cetuximab and related anti-epidermal growth factor receptor (EGFR) antibody therapies provide increased survival for patients, recent studies have revealed that the long-term clinical benefit may be limited (8). Despite meaningful responses in a small proportion (<20%) of HNSCC patients treated with immunotherapy (9,10), most patients fail to benefit from these drugs suggesting the continued need for alternative or combination approaches. The Cancer Genome Atlas (TCGA) report and related studies have revealed potentially targetable pathways, most prominently increased pro-proliferative signaling along the PI3K/AKT/mTORC axis driven primarily by gain of function activating mutation or amplification of PIK3CA, or loss of function of its negative regulator PTEN(11–15).

These findings have promoted the development of targeted therapeutics against PI3K/mTORC signaling. Over 30 active clinical trials in various phases are investigating PI3K inhibitors for head and neck cancer alone. Two recent entrants BYL719 and BKM120 have resulted in pre-clinical success with on-going trials in multiple solid tumor indications including HNSCC(16–18). While promise remains for PI3K inhibitors, to date there have not been any major clinical successes(19). An alternative point at which to impact this pathway is further downstream at the mTORC signaling node. The clinical use of rapamycin and the derivative rapalogs was among the first class of targeted agents to be used in the treatment of cancer. While there are currently a number of trials evaluating rapamycin, everolimus, and temsirolimus; to date there have been no major successes in the treatment of HNSCC(20). More recent efforts have focused on ATP competitive kinase inhibitors targeting either both PI3K/mTORC or the dual mTORC complexes. As these compounds target the catalytic site of mTOR, they impact both the AKT phosphorylation function of the Rictor containing mTORC2 complex, and the protein translation function of the raptor containing mTORC1 complex(21). The preferred targeting approach remains uncertain.

Herein, we utilized two hallmark compounds in this field, the PI3K/mTORC inhibitor NVP-BEZ-235 and the dual mTORC1/2 inhibitor AZD8055(18,22–27) to investigate their role in improving the response to cetuximab in HNSCC. While newer generations of both classes with improved toxicology profiles have emerged, the goal here was to evaluate these classes of compounds in the treatment of HNSCC both as single agents and in combination with the standard of care cetuximab. While initial reports had initially indicated that mutations or

other alterations along the PI3K/Akt/mTORC axis strongly predicted sensitivity to inhibitors targeting this pathway(12,28), more recent evidence suggests that this relationship is more complex(29,30), and that tumors both with and without such alterations may benefit from the addition of PI3K/mTORC to cetuximab treatment(16). In this work, we test both in vitro and in vivo HNSCC models containing both PI3K/Akt/mTORC altered and unaltered examples, to determine whether the addition of an ATP competitive kinase inhibitor can provide additional antitumor effects. Given the number of PI3K specific compounds that have already progressed to clinical trial, we focused our efforts on the dual PI3K/mTORC and dual mTORC classes as a precursor to follow on studies of these trials.

Materials and Methods

Additional details on all methods are included in the supplemental information.

Cell lines, strains, and drugs

Cell line (HPV-negative: UM-SCC1, and TU-138; HPV-positive: UD-SCC2, UM-SCC47, and UPCI-SCC90) sources and culture conditions are summarized in Table S1. UM-SCC1 and TU-138 were received in 2001 and 2006, respectively. All HPV-positive cell lines were obtained in 2010. The identity of all cell lines was confirmed via short-tandem repeat testing within 3 months of use (Supplemental data). AZD8055 and NVP-BEZ-235 were purchased from LC-Labs (Woburn, MA). Cetuximab (IMC-225, Erbitux) was purchased from the University of Wisconsin Hospital Pharmacy.

Growth inhibition assay

Cells were plated in 96-well plates and 24 hrs post-plating treated at indicated doses and incubated for 72–96 hrs. Every 24 hrs cells per well were determined using a SpectraMax i3 MiniMax 300 Imaging Cytometer plate reader using the optical imaging module and transmitted light setting. The Softmax-Pro v6.4 software was trained to automate counting of each cell type. This timecourse approach enabled the temporal analysis of cell proliferation; at 72 or 96 hrs when control wells were nearing confluency, treated wells were normalized to DMSO controls and IC50 values were calculated with GraphPad Prism v7 using the inhibitor concentration vs response (three parameter) function.

Clonogenic expansion assay

Cells were plated in 12-well plates, treated at indicated doses 24 hrs post plating, and allowed to incubate in media containing the inhibitors for 7 to 21 days, until DMSO control wells had colonies of 50 or more cells. Colonies were fixed, stained with methanol/crystal violet, and colonies of 50 or more cells were counted, surviving fraction was determined and plotted using Prism. Statistical comparisons were made via one-way ANOVA with Tukey’s multiple comparison test.

BrdU assay

Cells were plated in 96-well plates, 24 hrs post-plating treated at indicated doses, and allowed to incubate for 72–96 hrs. BrdU incorporation was measured and normalized to

DMSO control using a BrdU ELISA according to manufacturer instructions (Roche ref:11 647 229 001).

Apoptosis assay

Apoptosis was measured by caspase activity with the Caspase-Glo 3/7 assay (Promega #G8091) according to manufacturer instructions. Luciferase intensity was normalized to number of cells/well and expressed relative to DMSO controls.

Immunoblotting

Following treatment, cells were lysed with RIPA buffer supplemented with protease/phosphatase inhibitor cocktail (Cell Signaling Techonologies #5872) and sonicated. Equal amounts of protein were analyzed by SDS-PAGE (~50μg/well), transferred to polyvinylidene difluoride (PVDF) membranes (Immobilon-FL), probed by specific primary antibodies (Table S2) by overnight incubation at 4°C, and detected with NIR-conjugated secondary antibodies (LiCOR) imaged on a LiCOR Odyssey FC.

siRNA knockdown experiments

Cells were transfected in suspension at indicated concentrations of siRNA oligos (Table S3) using Lipofectamine RNAiMax (Life Technologies). For western blots, cells were incubated with siRNA for 72 hrs prior to harvest and processed as above. For proliferation assays, cells were analyzed as above.

Hotspot mutational analysis

Total genomic DNA was isolated from PDX FFPE tissue and HNSCC cell lines and sequenced using the Illumina TruSeq Cancer Amplicon panel and analyzed as described previously(31). Sequencing data has been deposited with the sequence read archive under BioProject ID: PRJNA381909.

Mice

Six to eight week old female NOD-SCID gamma (NSG, NOD.Cg-*Prkdc*^{scid} *Il2rg*^{tm1Wjl}/SzJ) mice (Jackson Laboratories) were used for PDX revival and tissue amplification; six to eight week old female Hsd:athymic Nude-*Foxn1*^{nu} (Harlan Laboratories) were used for therapy studies (32). Mice were kept in the Association for Assessment and Accreditation of Laboratory Animal Care-approved Wisconsin Institute for Medical Research (WIMR) Animal Care Facility. Animals were housed in specific pathogen free rooms, and their clinical health was evaluated weekly. Studies involving the mice were carried out in accordance with an animal protocol approved by the University of Wisconsin.

PDX cetuximab response studies

HNSCC PDXs were generated and propagated in our group as described previously(32,33). Ten models were evaluated for response to cetuximab by reanimating cryopreserved PDX tissue in NSG mice and then distributed to nude mice for therapy studies. Tumor volume was assessed twice weekly with Vernier calipers and calculated according to the equation $V = (\pi/6) \times (\text{large diameter}) \times (\text{small diameter})^2$; when average volume reached 250mm^3, mice

were randomized into control or cetuximab treatment, receiving cetuximab 2X/week at 10mg/kg by intraperitoneal injection(i.p.) for two weeks, vehicle mice received saline i.p. injections. Two weeks following treatment end, tumor size was measured and used to calculate treated/control (T/C) ratios using Prism.

PDX combination therapy studies

Mice were randomized into control (vehicle), AZD8055, cetuximab, or combination treatment groups (n=4–6 mice/10–16 tumors per group). AZD8055 was formulated in 30% Capsitol and delivered once daily at 20mg/kg by oral gavage(p.o.) as described previously (22). Cetuximab was dosed twice weekly at 10mg/kg i.p. Vehicle and single treatment mice received 30% Capsitol p.o. or saline i.p. as appropriate. At times indicated post-treatment, additional tumor-bearing mice were sacrificed and tumors were harvested for FFPE. Growth curves were statistically evaluated with the non-parametric Friedman's test using Prism.

Histology and immunohistochemisry

FFPE preserved PDX tissue was microtomed for 5μm sections and stained with H&E or IHC for indicated targets (Table S1) as described previously (34).

Results

Characterization of HNSCC PDX and cell line models identifies potential mTORC inhibition targets

We characterized an array of in vivo and in vitro HNSCC models, analyzing potential genetic and protein biomarkers, and evaluating therapeutic response to the current standard of care targeted agent, cetuximab. We have previously described the establishment and other characteristics of our cohort of PDX models(31–33); here we show hotspot mutational profiling using an Illumina cancer targeted sequencing panel, with key genes and patient demographic data highlighted in Figure 1A. We identified two PDXs in our cohort containing PIK3CA helical-domain activating mutations, as well as a range of PTEN expression levels as analyzed by IHC (Figure 1A and S1). We subjected approximately half of the cohort to in vivo cetuximab treatment studies using a flank subcutaneous approach. Response was evaluated as durable growth delay for cetuximab treated relative to control mice (T/C ratio) and were plotted from least to most responsive. These growth delay responses were then highlighted by HPV status and potentially impactful alterations (Figure 1B). Neither HPV status nor mutation profile correlated with response to cetuximab. This preliminary work was used to select models with a potential mTORC-inhibitor targetable alteration or high intrinsic cetuximab resistance for further investigation. Five established HNSCC cell lines were subjected to the same targeted sequencing panel (Figure 1C). While no obvious impactful mutations were identified, UPCI-SCC90 was shown to have amplified PIK3CA and resulting pathway activation including high levels of pAKT_S473 and p-p70S6K_T389, consistent with previous reports(35). This characterization enabled proper selection of model PDXs and cell lines for investigation of mTORC and EGFR inhibition.

mTORC inhibition had greater anti-proliferative effect than EGFR inhibition on HNSCC cells

We evaluated the same panel of HNSCC immortalized cell lines (Figure 1C), including 3 HPV+ (UD-SCC2, UM-SCC47, and UPCI-SCC90) and 2 HPV− (UM-SCC1 and TU-138), for response to the dual mTORC1/2 inhibitor AZD8055, the mTORC/PI3K inhibitor NVP-BEZ-235, and cetuximab. Growth inhibition was assayed by an automated cell counting based proliferation assay (Figure 2A). Cell proliferation was assayed every 24 hours over 72–96 hours of growth in drug, the resulting growth curves revealed a slower growth rate with increasing drug concentration, but no loss of cell numbers suggesting an anti-proliferative rather than cell killing effect (Figure S2). The cell lines displayed a fairly uniform response to both AZD8055 (3-fold difference highest to lowest in IC50 value) and NVP-BEZ-235 (3-fold difference highest to lowest in IC50 value) as shown in Table 1. Cell lines identified to have PIK3CA amplification (UPCI-SCC90) or PTEN copy loss (UD-SCC2), had generally lower AZD8055 IC50 values, but did not reach statistical significance ($p=0.16$). Differences in inhibition to the dual PI3K/mTORC inhibitor NVP-BEZ-235 were even more muted across the five cell lines (Figure 2A). Response to cetuximab treatment was barely discernable in this assay: IC50 values could not be calculated for any of the cells lines with a sufficiently good fit ($R^2>0.75$). Conversely we were able to discern a response to cetuximab using a clonogenic expansion assay, leading us to employ this assay for all three therapeutics (Figure 2B). We observed a similar level of response to both small molecule inhibitors across the five cell lines, but this assay revealed differences in their ability to grow in the presence of cetuximab; the HPV+ cell lines demonstrated a dose dependent response to this agent while the HPV− cell lines, UM-SCC1 and Tu-138, presented more modest responses to cetuximab and TU-138. Immunoblot analysis demonstrated that neither EGFR nor pEGFR expression predicted for cetuximab response (Figure 1D).

To investigate the mechanism of the inhibitors' effects we used a BrdU uptake assay to show that cell division correlated with growth inhibition (Figure 2C). For example, UMSCC-47 was among the more responsive cell lines to AZD8055 in the clonogenic expansion assay, at 10nM concentration about 10% of cells were able to proliferate, and concordantly the BrdU uptake was approximately 20% of control. Conversely at those same concentrations, TU-138 both had more BrdU uptake and less growth inhibition. We next investigated the induction of apoptosis using a Caspase 3/7 luciferase assay. While caspase activity was elevated for some cell lines at high drug concentrations, little if any induction of apoptosis was observed for any of the three drugs (Figure 1D) at concentrations near their IC50 values. These results demonstrate that both dual mTORC and mTORC/PI3K inhibitors had a greater anti-proliferative effect on HNSCC cells than cetuximab and suggest that the mechanism is growth suppression rather than induction of cell death.

Combination of cetuximab with mTORC/PI3K inhibition effectively blocks signaling pathways but provides little additional growth inhibition

We next investigated whether the combination of the FDA-approved targeted therapy for HNSCC, cetuximab, with either AZD8055 or BEZ-235 showed any additive effects on cell proliferation. We selected the clonogenic expansion assay to perform this test as it was more effective in revealing differences in monotherapy. With the exceptions of TU-138 and UPCI-

SCC90 there was little if any additional anti-proliferative effect when 100nM cetuximab was added to either small molecule agent (Figure 3). Immunoblots confirmed that each inhibitor was effectively suppressing its molecular target. In a dose dependent manner both AZD8055 and BEZ-235 inactivated the mTORC2 target AKT and the mTORC1 target 4EBP1, as evidenced by decreased phosphorylated protein. Cetuximab inhibited phospho-EGFR and two downstream targets AKT and MAPK1, but had less effect on further members of the AKT/mTORC signaling arm as shown by relatively normal levels of p4EBP1 and pS6. Effective inactivation of downstream members of this signaling arm correlated with decreased cell survival (Figure 3, immunoblot panels). The combination of the monoclonal antibody with a small molecule inhibitor produced effective inactivation of both p4EBP1 and pMAPK1, but with the exception of TU-138 and UPCI-SCC90 produced little additional reduction in survival.

mTORC or PI3K plus EGFR knock down reveals similar anti-proliferative effects

In order to confirm the pharmacological effects, we utilized a specific siRNA knock-down(KD) approach against mTOR, PIK3CA, and EGFR to inhibit these signaling pathways in the same HNSCC cell lines. Effective knockdown was confirmed by immunoblotting (Figure 4). MTOR and PIK3CA was also evaluated in combination with EGFR KD. Functional effects of the knockdown were assessed by a growth inhibition assay. While results varied across the different cell lines, knockdown of either mTOR or PIK3CA typically produced greater growth suppression than knockdown of EGFR. Combination knock down of EGFR with either other protein had minimal additive effects, similar to the results with the pharmacologic inhibitors. Overall, the results of the siRNA experiments suggest that suppression of targets in the PI3K/AKT/mTORC arm of EGFR signaling are more effective at reducing HNSCC cell growth and survival than directly targeting EGFR.

EGFR/mTORC combination therapy evaluated in selected PDX models

Previous work has suggested important differences between in vitro and in vivo models in response to EGFR and PI3K inhibitors, where effects seen in one system may not be observed in the other (36,37). To address these concerns and to expand our efforts to a more clinically relevant model system, we evaluated the combination of these therapeutic agents in five of the ten PDX models. PDXs were selected on the basis of PIK3CA activating mutation (UWSCC-6 and 13) or for intrinsic cetuximab resistance (UWSCC-1, 17, and 64). Mice were treated with daily administration of the dual mTORC inhibitor AZD8055 by oral gavage and bi-weekly dosing of i.p. cetuximab or single agent therapy for comparison for two or three weeks (Figure 5A). Pharmacokinetic (PK) analysis performed in the initial characterization of AZD8055 demonstrated that dose we selected (20mg/kg QD) produces free serum concentrations of drug of approximately 100nM, similar to the levels we tested in vitro(22). The combination therapy produced a significant growth delay in all five tumor models (repeated measures Friedman’s test, p-value at least <0.05), while either agent given alone was often ineffective at slowing tumor growth, suggesting at least an additive effect of the combination therapy. Mouse masses were recorded during and following treatment, no weight loss or other adverse effects were observed (Figure S3). Molecular target inhibition was confirmed by immunohistochemical analysis of FFPE tissues harvested 2 hrs post initial treatment. Primary drug targets were inhibited as expected (Figure S4). The most robust

inhibition was observed at downstream signaling indicators pMAPK1 and p4EBP1 which were effectively inhibited by cetuximab and AZD8055, respectively. While for the majority of tumor models we had only sufficient mice for early post-treatment tumor harvesting, for UWSCC-64 we were able to sacrifice mice at the conclusion of two weeks of treatment. These FFPE tissues were analyzed by Ki-67 and cleaved Caspase3 IHC. (Figure 5B). Only the combination therapy produced a statistically significant reduction in Ki-67+ cells (one-way ANOVA, Tukey's multiple comparisons test, $p<0.05$). No significant difference between the four arms of the study were seen in cleaved-caspase staining, consistent with anti-proliferative rather than pro-apoptotic mechanism of drug action. Overall, we observed a greater benefit of combining mTORC inhibition with anti-EGFR therapy in the in vivo PDX models than we did in cell lines.

Discussion

In this study, we evaluated in vitro and in vivo models of HNSCC for response to mTORC inhibition both alone and in combination with cetuximab, to establish a pre-clinical basis for whether a catalytic mTORC inhibitor could be a potentially effective addition to cetuximab in HNSCC. While both rapalogs and PI3K inhibitors are being evaluated in HNSCC, there has been only limited investigation of the particular combination of an ATP competitive mTORC small molecule inhibitor with cetuximab. A key component of this work is the identification and validation of predictive biomarkers that would guide the selection of patients to this therapeutic combination. While the goal of biomarker selection has been extensively investigated, our work here adds to the growing complexity and perhaps tenuous linkage between biomarker and treatment.

We began by evaluating a molecularly characterized panel of HPV+ and HPV− HNSCC cell lines for response to a dual mTORC1/2 (AZD8055) and a PI3K/mTORC (NVP-BEZ-235) inhibitor. Despite the presence potentially impactful alterations such as PIK3CA amplification (UPCI-SCC90) or PTEN copy loss (UD-SCC2) the response to either inhibitor was fairly uniform with a less than 5-fold difference in IC50 values. Timecourse analysis of the growth inhibition assay used to generate the IC50 calculations, demonstrated that increasing drug concentration only slowed cell growth and did not reduce the number of cells, even at micromolar concentrations. We further investigated the mechanism of inhibition of these compounds contrasting a DNA replication assay with a caspase activity based apoptosis assay, and found little if any caspase activity. Conversely changes in DNA replication were in the same direction and to the order of magnitude approximated functional growth inhibition, suggesting an anti-proliferative rather than pro-death action of these drugs.

We next evaluated combination treatment using the clonogenic expansion assay as due to better detection of cetuximab inhibition with this assay. Despite the observation that single and combined treatments inhibited the molecular targets as expected (i.e. AZD8055 reduced phosphorylated AKT and S6; cetuximab reduced pEGFR and pMAPK1), little additive benefit of the combination was apparent. Indeed, suppression along the PIK3CA/AKT/mTORC axis appeared to play the dominant role and was almost sufficient to inhibit growth

and proliferation by itself. Specific siRNA knock-down of mTOR or PIK3CA, either solely or in combination with EGFR mirrored these effects

Despite minimal additional benefit of combining an mTORC inhibitor with cetuximab in vitro, previous studies have shown that the response to cetuximab can be much more pronounced in vivo (38,39). In our panel of HNSCC PDXs we observed a range of responses to cetuximab treatment. Surprisingly, neither HPV status nor putative mutational or protein biomarkers predicted for response. We selected five of these models for an AZD8055/cetuximab combination study, two that contain well described PIK3CA activating mutations and three that presented high intrinsic resistance to cetuximab. The PDXs containing PIK3CA activating mutations were chosen to mimic the approach used in the ongoing NCI-Molecular Analysis for Therapy Choice (NCI-MATCH-NCT02465060) study investigating precision oncology using a large sequencing based “basket” trial. Combination therapy resulted in improved tumor control in all 5 models tested and slowed growth even in those models in which single agent therapy showed no response. Unfortunately, anticipated predictive markers were not confirmed. UWSCC-6 containing the PIK3CA E545K mutation was highly responsive to both the mTORC monotherapy and combination therapy. After completing treatment this tumor regrew rapidly, suggesting that this mutation was a major driving force in the growth of this tumor. Conversely, UWSCC-13, which was identified with a related PIK3CA helical domain mutation (E452K) did not respond at all to single agent AZD8055, but was dramatically suppressed by the combination therapy, with durable growth delay at almost 30 days post end of treatment. Of the three PIK3CA WT tumors, two presented poor response to single agent and had only marginal improvement on combination therapy, while the third UWSCC-64, was among our best responders to the dual treatment. While the combination therapy improved response in all five models, the level of improvement varied from model to model. While the molecular targets of each treatment were inhibited in all five tumors, there did not appear to be a strong correlation between pre-treatment levels of likely protein biomarkers and response.

Taken together these results highlight the complexity in attempting to match therapy to molecular markers that predict for response, and that the presence of a single expected marker rarely functions as a binary switch. While early reports in the targeting of the PI3K pathway suggested that such divergent effects could be observed, they perhaps are more the exception than the typical response. In the landmark paper Lui and co-authors found that a HNSCC patient derived xenograft with the PI3KCA E545K mutation was supremely responsive to NVP-BEZ-235 while a WT model was completely non-responsive(12). However, when evaluated in the context of hundreds of PDX models PIK3CA or PTEN mutation alone was not predictive of a response to the PI3K inhibitor, BYL719 (29). While PI3KCA mutation combined with WT PTEN was indicative of higher activity (2/3 responding), a large number of models were required to observe this effect. In the context of the limited number of patients typically evaluated in a Phase I or II trial such differences may be difficult to detect. While one trial of BYL719 (NCT01219699) and several of BKM120 (NCT01570296, NCT01572727, NCT01833169) have utilized PI3K status as a stated inclusion or stratification criteria, none specific to HNSCC has yet been registered, potentially due to recruitment concerns.

The retrospective analysis of genomic markers in HNSCC clinical trials investigating PI3K inhibitors the record has also not been compelling. The addition of the pan-PI3K isoform inhibitor PX-866 to cetuximab in patients with recurrent metastatic HNSCC did not confer any response benefit including four patients who had PIK3CA helical domain activating mutations(30). Similarly, the addition of the rapalog everolimus to erlotinib treatment did not induce a durable response in a patient with a PIK3CA H1047R mutation (40). While larger trials with the genomic biomarker selection criteria designed as a critical component of the study, such as the NCI-MATCH, are likely to bear more successful results, in the more limited scale of a typical Phase II trial such conclusions will likely be challenging to draw. Similarly, researchers using PDXs and other clinical sample derived models must strive to design studies with adequate number of well characterized models that recapitulate the likely patient population as well as possible. Researchers should also seek to adhere to the reporting standards required in the publication of clinical trials, including releasing the information on all models tested and avoiding highlighting the exceptional responders as indicative of a typical outcome.

While responses varied from model to model, a general trend observed in our work was the small magnitude of additional growth suppression when cetuximab was added to AZD8055 in the five established HNSCC cell lines tested. In contrast, in all five PDX models, the combination therapy was more effective than either treatment alone. Several factors may in part explain these differences: cell autonomous effects resulting in greater suppression of downstream signaling, tumor-stroma crosstalk that is not recapitulated using standard in vitro culture approaches, or anti-tumor effects of ADCC in vivo (even within an immune compromised model). While the immunodeficient nude mouse is far from an ideal model for the study of antitumor immunity, these animals do produce NK cells (41) and have been used to study the role of ADCC using tumor-specific antibodies(42). We looked for tumor infiltrating immune cells by morphological analysis of H&E stained slides and CD45 IHC in cetuximab and control treated animals. This revealed few if any immune cells and no differences when comparing treatments groups. While molecular target inhibition by drug was similar in both in vitro and in vivo models, we were limited in the timepoints post-treatment for the PDXs that could be assayed. It is possible that signaling differences arose at later time scales that could explain the additive response in PDXs. More likely however, is the more complex biology of the mouse model with interaction of the tumor with the stromal and vascular system of the mouse that contributed to this difference. Systemic administration of these therapeutics may well induce changes to the tumor microenvironment that impact tumor growth, but are completely absent from standard in vitro monoculture. We are currently developing both orthotopic and humanized mouse models which engraft a functional immune system for use with our PDX system, as well as microscale devices that allow for in vitro co-culture of tumor and stromal cells. These developments will enable a more robust investigation of immune and tumor microenvironment mediated effects.

While the PDX engrafted on an immunocompromised animal may represent a poor model for the study of immune anti-tumor biology it does serve as a more direct approach for the investigation of tumor signaling biology, without the potential confounding effects of the immune response. Our results showed that while suppression of PI3K/AKT/mTORC signaling was largely sufficient to inhibit proliferation of HNSCC cells in vitro, it had only

limited effect on xenograft tumors in vivo. However, suppression of both PI3K/AKT/mTORC signaling and RAS/RAF/MAPK1 signaling by the combination of AZD8055 with cetuximab resulted in dramatic growth suppression. Consistent with the function of these compounds, this effect was anti-proliferative rather than pro-apoptotic and highlights the potential for combination with cytotoxic therapy such as radiation or immunotherapy.

Considering the well-trod ground on which this work rests, the true clinical potential of this approach must be carefully considered. Two PI3K specific inhibitors BKM120 and BYL719 are currently under clinical evaluation for HNSCC as both monotherapy and in combination with cetuximab. The mTORC rapalog everolimus is under similar study. However, several PI3K inhibitors have already been investigated in this setting with only limited clinical success, suggesting that targeting an alternative node in this signaling pathway may be worthy of further study. The catalytic mTORC inhibitors may well prove to be an attractive alternative and while the drug used in this work, AZD8055, is no longer under active clinical investigation, its next generation version AZD2014(43,44) is under study for multiple solid tumor types (NCT02599714, NCT02583542, NCT02064608) and could be investigated in HNSCC. While the ability to match therapy to a given biomarker profile remains challenging, the results of our study show that such a combination may have potential clinical benefit regardless of mutation or other alteration status.

The larger question facing targeted therapeutics using monoclonal antibodies (chimeric or fully humanized) or kinase inhibitors is their value in the context of the growing research and clinical success of checkpoint inhibitors and other immunotherapies. The approval of pembrolizumab and nivolumab for the treatment of recurrent/metastatic HNSCC in the 2016 represents the most dramatic improvement for treatment of these patients in almost a decade, and likely will come to form the standard of care treatment for many patients. However, while retrospective analysis of the Keynote-012 trial demonstrated that patients with high PD-L1 expression had greatly improved overall survival (~10 months) compared to single agent cytotoxic chemotherapy, those with low PD-L1 had only 5 months OS, roughly the same as cetuximab monotherapy in the recurrent/metastatic setting (10,45,46). Similarly, in the nivolumab Phase III trial (CheckMate 141), PD-L1 low patients had only marginal improvement in survival relative to standard monotherapy options(9). Based on the subset analysis of these patients with low PD-L1 expression, this cohort may well have greater benefit of adding an ATP competitive mTORC inhibitor to a cetuximab course rather than receiving a checkpoint inhibitor. Taken together, the response rate in these trials was 18% to pembrolizumab(10) and 13% to nivolumab(9). Clearly there is room for improvement. The data presented here suggests that the potential benefits of targeted therapy in the majority of HNSCC patients who do not benefit from immunotherapy remains promising.

Supplementary Material

Refer to Web version on PubMed Central for supplementary material.

Acknowledgments

We thank Aasta Pandey, Grace Blitzer, Molly Smith, Andrew P. Stein, and Dana Gunderson for additional experimental assistance. We would like to thank Ella Ward and University of Wisconsin Research Pathology facility

for tissue processing and histology services. We also would like to acknowledge the University of Wisconsin Translational Research Initiatives in Pathology laboratory, in part supported by the UW Department of Pathology and Laboratory Medicine and UWCCC grant P30 CA014520, for use of its facilities and services. The authors thank the University of Wisconsin Biotechnology Center DNA Sequencing Facility for providing the hotspot sequencing facilities and services.

Financial support and disclosures: Supported in part by R00 CA160639 (RJK), Department of Human Oncology Seed Grant (RJK), PhRMA Foundation Postdoctoral Fellowship in Translational Medicine and Therapeutics(ADS), the University of Wisconsin Carbone Cancer Center Support Grant P30 CA014520, the UW School of Medicine and Public Health through the Wisconsin Partnership Program, and Wisconsin Head and Neck SPORE Grant (NIH P50 DE026787).

References

1. Cancer Facts and Figures 2016. Atlanta: American Cancer Society; 2016.
2. Fakhry C, Zhang Q, Nguyen-Tan PF, Rosenthal D, El-Naggar A, Garden AS, et al. Human papillomavirus and overall survival after progression of oropharyngeal squamous cell carcinoma. J Clin Oncol. 2014; 32(30):3365–73. [PubMed: 24958820]
3. Ang KK, Harris J, Wheeler R, Weber R, Rosenthal DI, Nguyen-Tân PF, et al. Human papillomavirus and survival of patients with oropharyngeal cancer. N Engl J Med. 2010; 363(1):24–35. [PubMed: 20530316]
4. Chaturvedi AK, Engels EA, Anderson WF, Gillison ML. Incidence trends for human papillomavirus-related and -unrelated oral squamous cell carcinomas in the United States. J Clin Oncol. 2008; 26(4):612–9. [PubMed: 18235120]
5. Stein AP, Saha S, Yu M, Kimple RJ, Lambert PF. Prevalence of human papillomavirus in oropharyngeal squamous cell carcinoma in the United States across time. Chem Res Toxicol. 2014; 27(4):462–9. [PubMed: 24641254]
6. Bonner JA, Harari PM, Giralt J, Azarnia N, Shin DM, Cohen RB, et al. Radiotherapy plus cetuximab for squamous-cell carcinoma of the head and neck. N Engl J Med. 2006; 354(6):567–78. [PubMed: 16467544]
7. Bonner JA, Harari PM, Giralt J, Cohen RB, Jones CU, Sur RK, et al. Radiotherapy plus cetuximab for locoregionally advanced head and neck cancer: 5-year survival data from a phase 3 randomised trial, and relation between cetuximab-induced rash and survival. Lancet Oncol. 2010; 11(1):21–8. [PubMed: 19897418]
8. Ang KK, Zhang Q, Rosenthal DI, Nguyen-Tan PF, Sherman EJ, Weber RS, et al. Randomized phase III trial of concurrent accelerated radiation plus cisplatin with or without cetuximab for stage III to IV head and neck carcinoma: RTOG 0522. J Clin Oncol. 2014; 32(27):2940–50. [PubMed: 25154822]
9. Ferris RL, Blumenschein G, Fayette J, Guigay J, Colevas AD, Licitra L, et al. Nivolumab for Recurrent Squamous-Cell Carcinoma of the Head and Neck. N Engl J Med. 2016; 375(19):1856–67. [PubMed: 27718784]
10. Chow LQ, Haddad R, Gupta S, Mahipal A, Mehra R, Tahara M, et al. Antitumor Activity of Pembrolizumab in Biomarker-Unselected Patients With Recurrent and/or Metastatic Head and Neck Squamous Cell Carcinoma: Results From the Phase Ib KEYNOTE-012 Expansion Cohort. J Clin Oncol. 2016
11. Li H, Wawrose JS, Gooding WE, Garraway LA, Lui VW, Peyser ND, et al. Genomic analysis of head and neck squamous cell carcinoma cell lines and human tumors: a rational approach to preclinical model selection. Mol Cancer Res. 2014; 12(4):571–82. [PubMed: 24425785]
12. Lui VW, Hedberg ML, Li H, Vangara BS, Pendleton K, Zeng Y, et al. Frequent mutation of the PI3K pathway in head and neck cancer defines predictive biomarkers. Cancer Discov. 2013; 3(7): 761–9. [PubMed: 23619167]
13. Network CGA. Comprehensive genomic characterization of head and neck squamous cell carcinomas. Nature. 2015; 517(7536):576–82. [PubMed: 25631445]
14. Iglesias-Bartolome R, Martin D, Gutkind JS. Exploiting the head and neck cancer oncogenome: widespread PI3K-mTOR pathway alterations and novel molecular targets. Cancer Discov. 2013; 3(7):722–5. [PubMed: 23847349]

15. Stransky N, Egloff AM, Tward AD, Kostic AD, Cibulskis K, Sivachenko A, et al. The mutational landscape of head and neck squamous cell carcinoma. Science. 2011; 333(6046):1157–60. [PubMed: 21798893]
16. Lattanzio L, Tonissi F, Monteverde M, Vivenza D, Russi E, Milano G, et al. Treatment effect of buparlisib, cetuximab and irradiation in wild-type or PI3KCA-mutated head and neck cancer cell lines. Invest New Drugs. 2015; 33(2):310–20. [PubMed: 25603975]
17. Keam B, Kim S, Ahn YO, Kim TM, Lee SH, Kim DW, et al. In vitro anticancer activity of PI3K alpha selective inhibitor BYL719 in head and neck cancer. Anticancer Res. 2015; 35(1):175–82. [PubMed: 25550549]
18. Maira SM, Pecchi S, Huang A, Burger M, Knapp M, Sterker D, et al. Identification and characterization of NVP-BKM120, an orally available pan-class I PI3-kinase inhibitor. Mol Cancer Ther. 2012; 11(2):317–28. [PubMed: 22188813]
19. Cai Y, Dodhia S, Su GH. Dysregulations in the PI3K pathway and targeted therapies for head and neck squamous cell carcinoma. Oncotarget. 2017
20. Geiger JL, Bauman JE, Gibson MK, Gooding WE, Varadarajan P, Kotsakis A, et al. Phase II trial of everolimus in patients with previously treated recurrent or metastatic head and neck squamous cell carcinoma. Head Neck. 2016
21. Laplante M, Sabatini DM. mTOR signaling in growth control and disease. Cell. 2012; 149(2):274–93. [PubMed: 22500797]
22. Chresta CM, Davies BR, Hickson I, Harding T, Cosulich S, Critchlow SE, et al. AZD8055 is a potent, selective, and orally bioavailable ATP-competitive mammalian target of rapamycin kinase inhibitor with in vitro and in vivo antitumor activity. Cancer Res. 2010; 70(1):288–98. [PubMed: 20028854]
23. Rodrik-Outmezguine VS, Chandarlapaty S, Pagano NC, Poulikakos PI, Scaltriti M, Moskatel E, et al. mTOR kinase inhibition causes feedback-dependent biphasic regulation of AKT signaling. Cancer Discov. 2011; 1(3):248–59. [PubMed: 22140653]
24. Brachmann SM, Hofmann I, Schnell C, Fritsch C, Wee S, Lane H, et al. Specific apoptosis induction by the dual PI3K/mTor inhibitor NVP-BEZ235 in HER2 amplified and PIK3CA mutant breast cancer cells. Proc Natl Acad Sci U S A. 2009; 106(52):22299–304. [PubMed: 20007781]
25. Maira SM, Stauffer F, Brueggen J, Furet P, Schnell C, Fritsch C, et al. Identification and characterization of NVP-BEZ235, a new orally available dual phosphatidylinositol 3-kinase/mammalian target of rapamycin inhibitor with potent in vivo antitumor activity. Mol Cancer Ther. 2008; 7(7):1851–63. [PubMed: 18606717]
26. Naing A, Aghajanian C, Raymond E, Olmos D, Schwartz G, Oelmann E, et al. Safety, tolerability, pharmacokinetics and pharmacodynamics of AZD8055 in advanced solid tumours and lymphoma. Br J Cancer. 2012; 107(7):1093–9. [PubMed: 22935583]
27. Li Q, Song XM, Ji YY, Jiang H, Xu LG. The dual mTORC1 and mTORC2 inhibitor AZD8055 inhibits head and neck squamous cell carcinoma cell growth in vivo and in vitro. Biochem Biophys Res Commun. 2013; 440(4):701–6. [PubMed: 24103749]
28. Keysar SB, Astling DP, Anderson RT, Vogler BW, Bowles DW, Morton JJ, et al. A patient tumor transplant model of squamous cell cancer identifies PI3K inhibitors as candidate therapeutics in defined molecular bins. Mol Oncol. 2013; 7(4):776–90. [PubMed: 23607916]
29. Gao H, Korn JM, Ferretti S, Monahan JE, Wang Y, Singh M, et al. High-throughput screening using patient-derived tumor xenografts to predict clinical trial drug response. Nat Med. 2015; 21(11):1318–25. [PubMed: 26479923]
30. Jimeno A, Shirai K, Choi M, Laskin J, Kochenderfer M, Spira A, et al. A randomized, phase II trial of cetuximab with or without PX-866, an irreversible oral phosphatidylinositol 3-kinase inhibitor, in patients with relapsed or metastatic head and neck squamous cell cancer. Ann Oncol. 2015; 26(3):556–61. [PubMed: 25524478]
31. Swick AD, Stein AP, McCulloch TM, Hartig GK, Ong IM, Sampene E, et al. Defining the boundaries and expanding the utility of neck cancer patient derived xenografts. Oral Oncology. 2017; 64:65–72. [PubMed: 28024726]
32. Kimple RJ, Harari PM, Torres AD, Yang RZ, Soriano BJ, Yu M, et al. Development and characterization of HPV-positive and HPV-negative head and neck squamous cell carcinoma

tumorgrafts. Clinical cancer research : an official journal of the American Association for Cancer Research. 2013; 19(4):855–64. [PubMed: 23251001]

33. Stein AP, Saha S, Liu CZ, Hartig GK, Lambert PF, Kimple RJ. Influence of handling conditions on the establishment and propagation of head and neck cancer patient derived xenografts. PLoS One. 2014; 9(6):e100995. [PubMed: 24967635]
34. Stein AP, Swick AD, Smith MA, Blitzer GC, Yang RZ, Saha S, et al. Xenograft assessment of predictive biomarkers for standard head and neck cancer therapies. Cancer medicine. [Accepted November 18, 2014]
35. Martin D, Abba MC, Molinolo AA, Vitale-Cross L, Wang Z, Zaida M, et al. The head and neck cancer cell oncogenome: A platform for the development of precision molecular therapies. Oncotarget. 2014; 5(19):8906–23. [PubMed: 25275298]
36. Huang S, Armstrong EA, Benavente S, Chinnaiyan P, Harari PM. Dual-agent molecular targeting of the epidermal growth factor receptor (EGFR): combining anti-EGFR antibody with tyrosine kinase inhibitor. Cancer Res. 2004; 64(15):5355–62. [PubMed: 15289342]
37. Costa C, Ebi H, Martini M, Beausoleil SA, Faber AC, Jakubik CT, et al. Measurement of PIP3 levels reveals an unexpected role for p110β in early adaptive responses to p110α-specific inhibitors in luminal breast cancer. Cancer Cell. 2015; 27(1):97–108. [PubMed: 25544637]
38. Huang SM, Harari PM. Modulation of radiation response after epidermal growth factor receptor blockade in squamous cell carcinomas: inhibition of damage repair, cell cycle kinetics, and tumor angiogenesis. Clin Cancer Res. 2000; 6(6):2166–74. [PubMed: 10873065]
39. Huang SM, Bock JM, Harari PM. Epidermal growth factor receptor blockade with C225 modulates proliferation, apoptosis, and radiosensitivity in squamous cell carcinomas of the head and neck. Cancer Res. 1999; 59(8):1935–40. [PubMed: 10213503]
40. Massarelli E, Lin H, Ginsberg LE, Tran HT, Lee JJ, Canales JR, et al. Phase II trial of everolimus and erlotinib in patients with platinum-resistant recurrent and/or metastatic head and neck squamous cell carcinoma. Ann Oncol. 2015; 26(7):1476–80. [PubMed: 26025965]
41. Croy BA, Linder KE, Yager JA. Primer for non-immunologists on immune-deficient mice and their applications in research. Comp Med. 2001; 51(4):300–13. [PubMed: 11924787]
42. Morris ZS, Guy EI, Francis DM, Gressett MM, Werner LR, Carmichael LL, et al. In Situ Tumor Vaccination by Combining Local Radiation and Tumor-Specific Antibody or Immunocytokine Treatments. Cancer Res. 2016; 76(13):3929–41. [PubMed: 27197149]
43. Guichard SM, Curwen J, Bihani T, D'Cruz CM, Yates JW, Grondine M, et al. AZD2014, an Inhibitor of mTORC1 and mTORC2, Is Highly Effective in ER+ Breast Cancer When Administered Using Intermittent or Continuous Schedules. Mol Cancer Ther. 2015; 14(11):2508–18. [PubMed: 26358751]
44. Liao H, Huang Y, Guo B, Liang B, Liu X, Ou H, et al. Dramatic antitumor effects of the dual mTORC1 and mTORC2 inhibitor AZD2014 in hepatocellular carcinoma. Am J Cancer Res. 2015; 5(1):125–39. [PubMed: 25628925]
45. Vermorken JB, Trigo J, Hitt R, Koralewski P, Diaz-Rubio E, Rolland F, et al. Open-label, uncontrolled, multicenter phase II study to evaluate the efficacy and toxicity of cetuximab as a single agent in patients with recurrent and/or metastatic squamous cell carcinoma of the head and neck who failed to respond to platinum-based therapy. J Clin Oncol. 2007; 25(16):2171–7. [PubMed: 17538161]
46. Seiwert TY, Burtness B, Mehra R, Weiss J, Berger R, Eder JP, et al. Safety and clinical activity of pembrolizumab for treatment of recurrent or metastatic squamous cell carcinoma of the head and neck (KEYNOTE-012): an open-label, multicentre, phase 1b trial. Lancet Oncol. 2016; 17(7):956–65. [PubMed: 27247226]

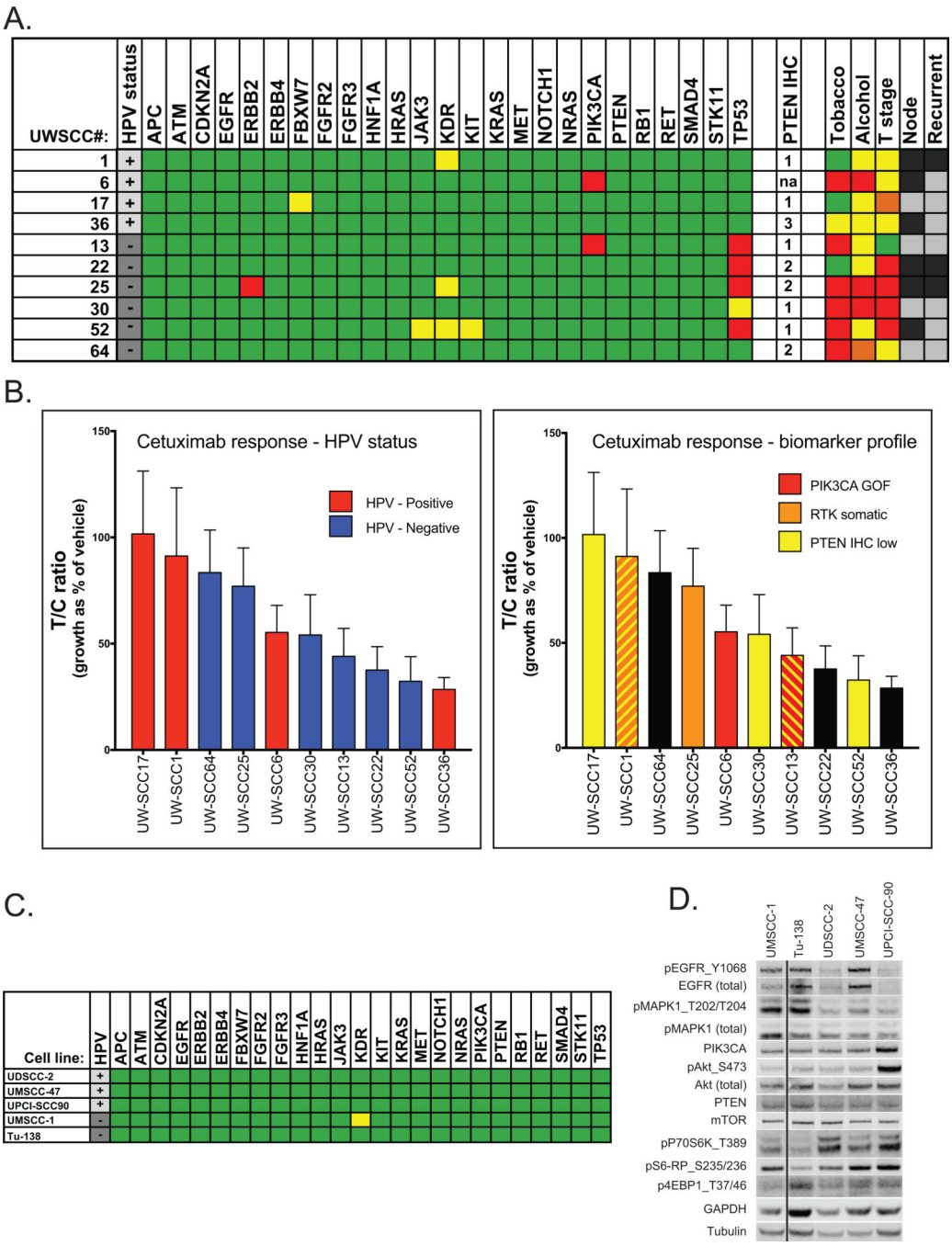

Figure 1. Characterization of HNSCC in vivo and in vitro models

A. HNSCC PDX cohort. HPV status: positive (+), negative (−). Genes assessed by mutational analysis. Green–no oncogenic mutation identified, yellow-previously reported oncogenic mutation in non-HNSCC cancer type, red-previously reported oncogenic mutation in HNSCC/major loss of function lesion detected. PTEN IHC: 1-low, 2-medium, 3-high, na-not evaluable. Tobacco use: green-never smoker, yellow-<20 pack years, red->20 pack years. Alcohol use: yellow-occasional, orange-moderate, red-heavy. T-stage: green-1, yellow-2, orange-3, red-4. Nodal involvement: black-positive, grey-negative. Recurrent:

black-recurrent, grey-primary. **B**. PDX cohort response to cetuximab treatment by T/C ratio. Tumors were highlighted by both HPV and mutational status. **C**. HNSCC cell lines. A. HPV: black-HPV+, grey-HPV−. Genes assessed by mutational analysis. Green–no oncogenic mutation identified, yellow-previously reported oncogenic mutation in non-HNSCC cancer type, red-previously reported oncogenic mutation in HNSCC/major loss of function lesion detected. D. Immunoblot of EGFR/AKT/PIK3CA/mTORC pathway proteins of HNSCC cells. WCL were harvested from cells grown in normal growth media. Lane 2 of this blot has been cropped and replaced by a solid line as it illustrates an unrelated cell line. The complete, unedited blot is shown in Figure S5.

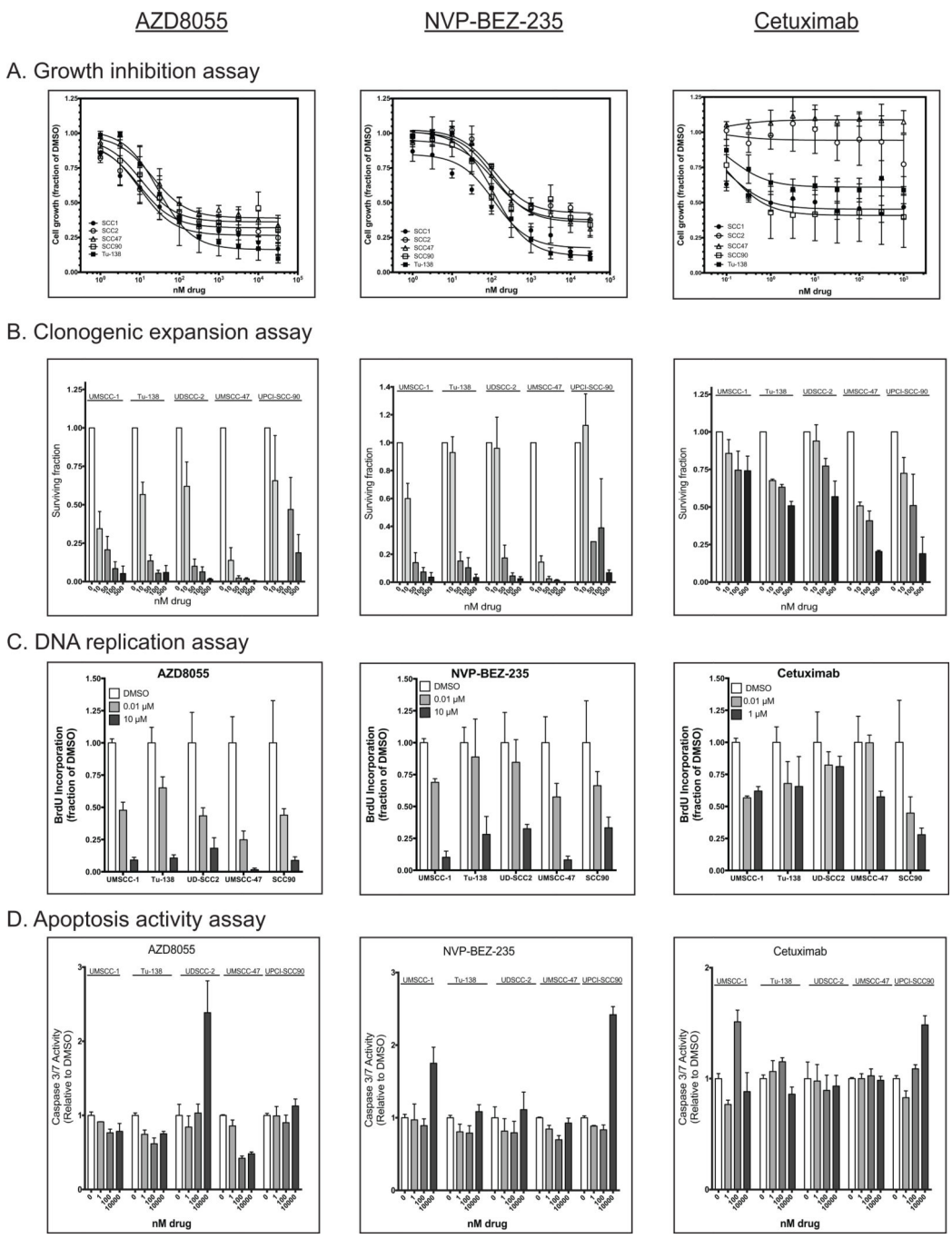

Figure 2. Effect of mTORC inhibitors and cetuximab on panel of HNSCC cell lines

A. Proliferation assay of AZD8055, BEZ-235, and cetuximab normalized to DMSO only control. HPV+ cell lines have open symbols; HPV− cell lines have closed symbols. Mean of three biological replicates with SEM error bars presented. **B**. Clonogenic expansion assay of panel of HNSCC cell lines with surviving fraction relative to DMSO for a given biological replicate. Mean surviving fraction of three biological replicates of quadruplicate wells shown. Error bar are SEM. **C**. DNA replication was measured by BrdU incorporation assay in the panel of HNSCC cells. Signal was normalized to DMSO controls, bars represent mean

of quadruplicate wells, error bars are SD. **D**. Apoptosis was measured via Caspase 3/7 activity in a luciferase based assay. Data represent mean values of triplicate wells, error bars are SD.

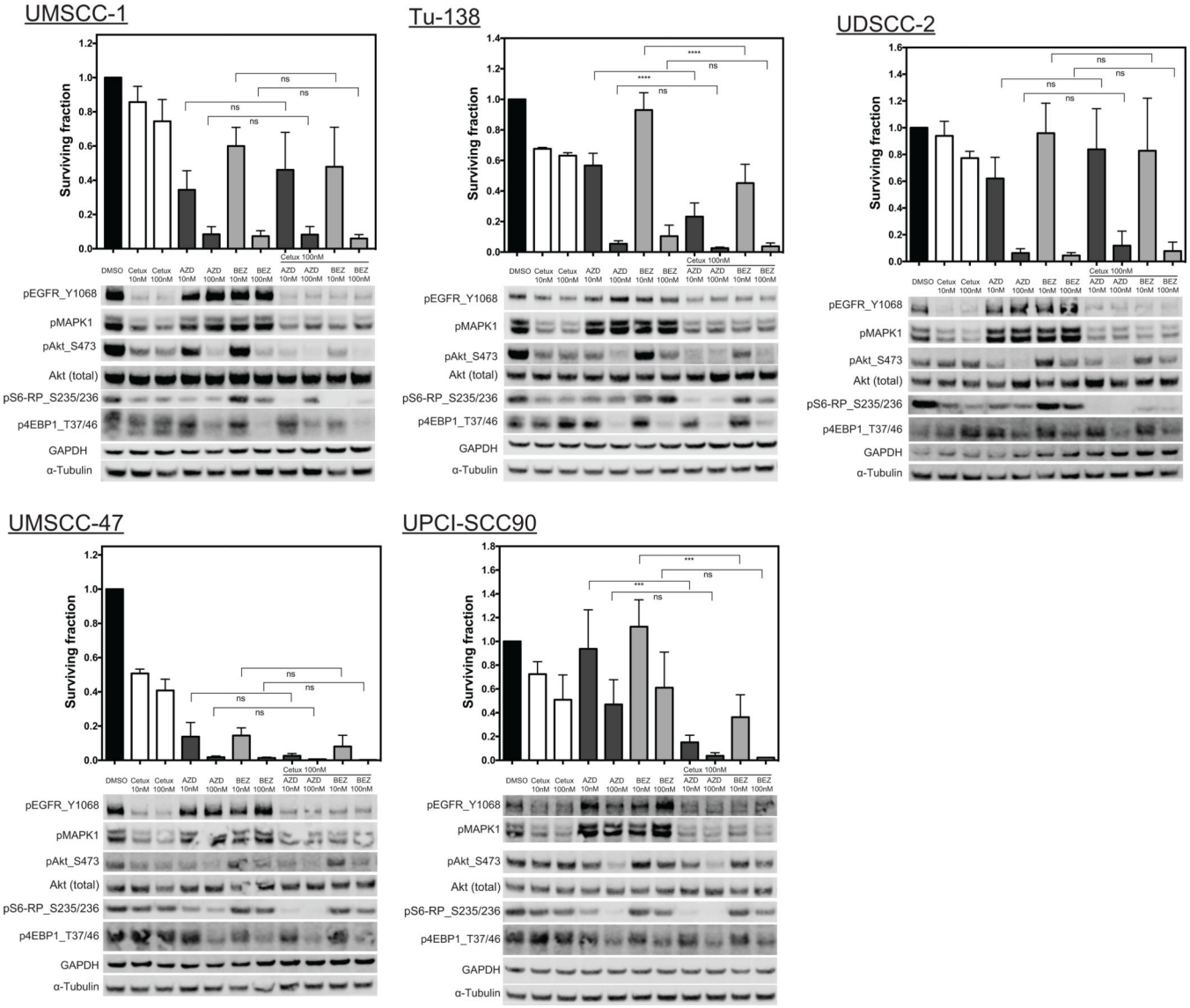

Figure 3. Immunoblotting of drug molecular targets with paired clonogenic expansion data

Panel of HNSCC cell lines was assayed for molecular targets of mTORC inhibitors and cetuximab by western blot after 2hrs of drug exposure. Paired clonogenic expansion data is shown above each immunoblot array, single drug treatments shown in Figure 2B are repeated here for ease of viewing adjacent to immunoblots and combination treatments. Bars present mean surviving fraction of three biological replicates of quadruplicate wells shown, error bar are SEM. Statistical comparison made with one-way AVOVA with Tukey's multiple comparison test; p-values: *<0.05, **<0.001, ***<0.0001, ****<0.00001, ns-not-significant.

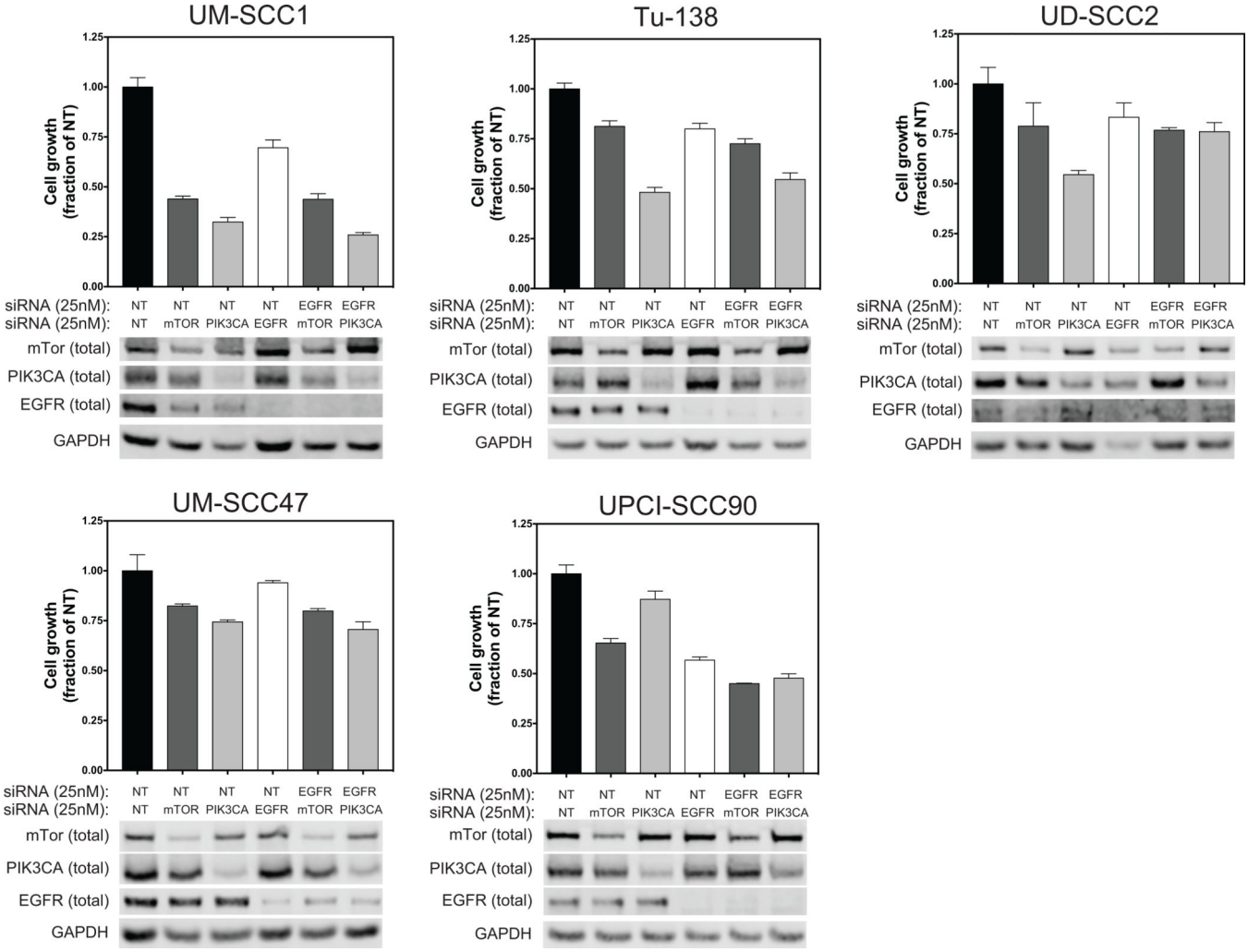

Figure 4. SiRNA knock-down of mTORC, PIK3CA, and EGFR in HNSCC cell lines

Bar plots- growth inhibition assay to assess growth impact of siRNA KD. NT – non-targeting siRNA. 72hrs post transfection, counts normalized to NT. Bars represent mean of triplicate wells, error bars are SD. Immunoblot of total protein of targeted genes a 72 hrs after siRNA transfection at 25nM.

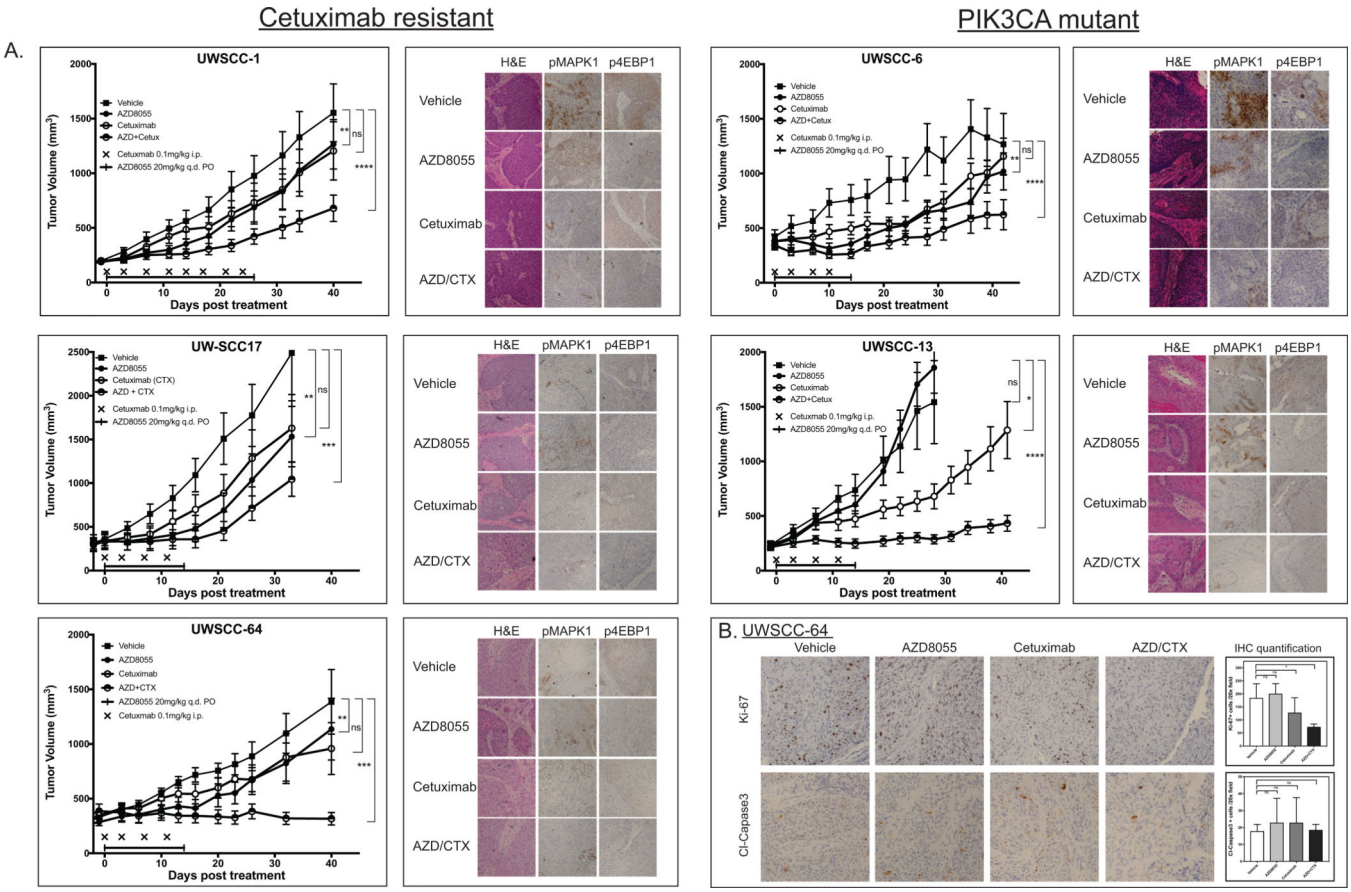

Figure 5. Combination mTORC/EGFR therapy of selected PDX models

A. Growth curves of five selected PDXs. Data points represent mean tumor volume (n=10–16 tumors/arm), error bars are SEM. Growth curves were compared over all days shown by repeated measures Friedman's test with Dunn's test for multiple comparison. P-values for Dunn's test results for vehicle to each treatment arm: *<0.05, **<0.001, ***<0.0001, ****<0.00001, ns-not-significant. Adjacent IHC panel present FFPE tissues harvested 2 hrs post initial treatment of indicated therapeutics. Images shown are representative 20X field of overall staining. **B**. Proliferation and apoptosis markers for UWSCC-64 at conclusion of 14 days of treatment. Top row- Ki-67 IHC staining. Bottom row cleaved caspase 3. Images shown are 20X representative fields of overall staining. Ki-67 or cleaved caspase 3 positive cells were manually counted by a blinded individual in 2 high powered fields for two independent tumors. Columns present mean positive cells/field with SD error bars. One-way ANOVA with Tukey's multiple comparison test was used to compare the different treatment arms (p-values: *<0.05, ns-not-significant).

Table 1

IC50 values for AZD8055, BEZ-235, and Cetuximab

Cell line	AZD8055 IC50 (nM)	95% CI	NVP-BEZ-235 IC50 (nM)	95% CI	Cetuximab IC50 (nM)	95% CI
UM-SCC1	10.0	4.8 to 21.9	44.2	20.0 to 100.5	nc	na
TU-138	29.3	13.4 to 66.0	135.0	74.5 to 246.2	nc	na
UD-SCC2	9.5	3.5 to 29.8	144.7	94.8 to 221.9	nc	na
UM-SCC47	20.7	12.5 to 34.6	133.2	65.6 to 278.8	nc	na
UPCI-SCC90	10.8	3.1 to 37.8	45.2	22.5 to 91.3	nc	na

nc – not calculated, na- not applicable